Physica A 168 (1990) 308–318
North-Holland

REMANENT MAGNETIZATION, LOWER CRITICAL FIELDS AND SURFACE BARRIERS IN AN $YBa_2Cu_3O_7$ CRYSTAL

M.W. McELFRESH[a], Y. YESHURUN[b], A.P. MALOZEMOFF[a] and F. HOLTZBERG[a]

[a]*IBM T.J. Watson Research Center, Yorktown Heights, NY 10598, USA*
[b]*Department of Physics, Bar-Ilan University, Ramat-Gan, Israel*

The isothermal remanent magnetization M_{rem} of an $YBa_2Cu_3O_7$ crystal was measured as function of the maximum applied field $10\,\text{Oe} \leq H_m \leq 40\,\text{kOe}$, for several isotherms $4.2\,\text{K} \leq T \leq 65\,\text{K}$, for $H_m \perp c$ and $H_m \| c$. Above an onset field for flux penetration H_p, M_{rem} initially increases sharply with H_m and then crosses over to a saturation value. An extended Bean model is used to fit the $M_{rem}(H)$ data. The derived onset field for $T > 50\,\text{K}$ is approximately linear with T and is in agreement with the lower critical fields $H_{c1}(T)$ measured by other techniques. At lower temperatures, however, H_p continues to increase. We incorporate surface barriers in the extended Bean model and consider the possibility that the low-temperature increase in H_p might be due to such barriers.

1. Introduction

The lower critical field H_{c1} has been studied in virtually all high-temperature superconductors by employing a variety of experimental techniques [1–11]. However, despite three years of extensive efforts, the anisotropic values of H_{c1} and, in particular their temperature dependence, are still controversial. Of particular interest is the recently reported behavior of H_{c1} in the temperature range $0 < T < 0.5T_c$, where, in contrast to expectations from conventional BCS models, which predict essentially no temperature dependence, $H_{c1}(T)$ was reported to rise strongly with decreasing temperature [9–11]. This is particularly surprising because H_{c1} is expected to be related to the temperature-dependent London magnetic penetration depth λ, roughly according to $H_{c1} = \phi_0 \ln \kappa / 4\pi\lambda^2$ (with ϕ_0 the flux quantum and κ the approximately temperature-independent ratio of penetration depth and coherence length). Yet λ has been observed by a couple of techniques [12–14] to be essentially temperature-independent for $0 < T < 0.5T_c$ implying a temperature-*independent* H_{c1} in this range.

All techniques used so far for measuring H_{c1} in the high-temperature superconductors involve identifying the onset of flux penetration at a field H_p.

A likely cause for erroneous determination of H_{c1} by such methods is the possible presence of a surface barrier, e.g. of the Bean–Livingston type [15]. In this paper we present new data on an $YBa_2Cu_3O_7$ crystal which confirm the anomalous temperature dependence of $H_p(T)$, and we present an analysis of these data which for the first time considers explicitly the possibility of a surface barrier contribution.

Two of the techniques previously used for determining H_{c1}, namely the study of deviations from linearity in the virgin magnetization curve [4], or the onset of flux penetration as a function of temperature in fixed field [5] are difficult to apply in the low-temperature range because large pinning makes these deviations and onsets difficult to define. Two other techniques, namely the study of the onset of flux creep [6] and of zero-field remanent moment as a function of applied field [7, 8] seem more promising in this range. However, as in all these experiments, onsets are difficult to define because of the seemingly inevitable smooth curvature in the onset region.

In this paper we apply the method of zero-field remanence onset to determine H_p, the field for onset of flux penetration, following Liu et al. [7] and Moshchalkov et al. [8], but introducing a critical state model to describe the full curve of remanence versus maximum applied field. This allows a more objective determination of the onset fields, which, it turns out, also show the anomalous temperature dependence reported earlier.

In section 2 we present the experimental results, in section 3 the critical state model and its fit to the data, and in section 4 a discussion of the implications for H_{c1}.

2. Experiment and results

The crystal used in this experiment is the same one as in ref. [5]. It has a rectangular shape of dimensions $537 \times 461 \times 162$ μm^3. Magnetic measurements have been carried out on a commercial Quantum Design SQUID magnetometer. The experimental procedure is the following: The sample is cooled in zero field from 100 K to the measurement temperature T. After stabilizing the temperature to better than 0.1 K a field H_m is turned on for 5 min. Then the field is turned off and the remanent magnetization $M_{rem}(H_m)$ is measured for an additional 5 min. The remanent values reported here are those measured at the end of the 5 min period. It should be noted, however, that in the interesting field range (i.e. near H_p) magnetic relaxation rates are relatively small and they have no significant effect on the data presented here. After taking the last M_{rem} the sample is warmed up to 100 K and the next measurement cycle is started. We emphasize that *each* point represents a full cycle from

the starting temperature 100 K to the measurement temperature, followed by increasing the field from zero to H_m and back again. Thus the data should not be confused with a virgin magnetization curve.

In figs. 1 and 2 we exhibit typical $M_{rem}(H_m)$ data, at several temperatures, for H both parallel and perpendicular to the c-axis. Qualitatively, all isotherms show similar features:

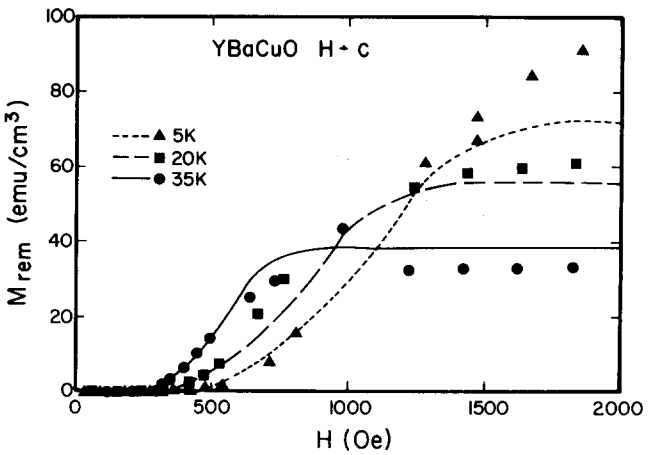

Fig. 1. Field dependence of the isothermal remanent magnetization for $H \perp c$ in an Y–Ba–Cu–O crystal for the various indicated isotherms. The lines are the results of the fit to eqs. (7), (9) and (10), with the parameters in table I.

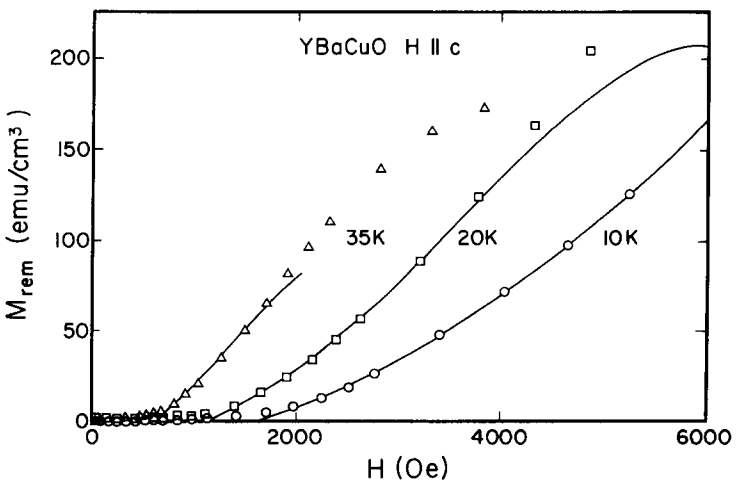

Fig. 2. Field dependence of the isothermal remanent magnetization for $H \| c$ in an Y–Ba–Cu–O crystal for the various indicated isotherms. Only the low-field data are shown here. The lines are the results of the fit to eq. (7), with the parameters in table II.

(i) In the low-field limit M_{rem} is virtually zero. Actually, for most isotherms, $M_{rem} \simeq 0.07\,\text{emu/cm}^3$ and $\simeq 0.11\,\text{emu/cm}^3$ for $H \perp c$ and $H \| c$ respectively, independent of H_m. This constant background is a result of the fact that the sample is cooled in a field of order 1 Oe, nominally zero field. When cooling in a field less than 0.1 Oe, the offset was eliminated without changing other features of the data. We therefore subtract this small offset in further analysis of the data.

(ii) With increasing maximum field H_m, M_{rem} increases rapidly with field. We call this region 1, and its onset point is what we call the experimental flux penetration onset field H_p.

(iii) Beyond an inflection point, $M_{rem}(H_m)$ enters a crossover regime which we call region 2 and whose indentification will become clearer in the theoretical section 3.

(iv) Finally, M_{rem} saturates; we call this region 3.

In fig. 2, we show the onset region in more detail. There is inevitable ambiguity in defining the onset point without some definition of the nature of the asymptotic approach of M_{rem} to zero with decreasing H_m. This will be the goal of section 3.

Finally, to test the possibility of a surface barrier effect on the onset regime, we performed a second study at a different magnet ramp rate. Observation of a shift with the 5× increased rate would indicate the presence of a surface barrier by reducing thermal activation over the barrier. We observed a null result, which unfortunately is inconclusive since we do not know a priori whether we are in an adequate time range to see a measurable effect.

3. Theory

In this section we calculate the remanent moment in a critical state model and compare the predictions to experimental data. In our model we take into account several effects which extend it beyond the simple initial formulation of Bean [16], and which have also been considered in the recent literature on high-temperature superconductors [5, 6, 17].

(1) We consider the critical current density J_c to depend on the local flux density $B(x)$, and we adopt a widely used form

$$J_c(B) = \frac{c}{4\pi} CB^{-n}, \tag{1}$$

where C and n can be functions of temperature and c is the speed of light, introduced to simplify later equations in cgs units.

(2) We include the effect of the lower critical field H_{c1} and the equilibrium magnetization. To do this, we approximate the Abrikosov equilibrium $B_{eq}(H)$ curve, which shows an infinite slope at H_{c1}, by a simple function, as proposed in recent publication [17]:

$$B_{eq} = 0 \quad \text{for } H < H_{c1}, \qquad B_{eq} = H - H_{c1} + H_b \quad \text{for } H > H_{c1}\,, \tag{2}$$

where H_b is the step height, which is a fraction of H_{c1}.

(3) We include the effect of a possible surface barrier to flux entry by using a "flux entry barrier" ΔH_{en} introduced by Clem [18], which shifts the surface boundary condition according to

$$H = H_a - \Delta H_{en}\,, \tag{3}$$

where H_a is the externally applied field (corrected for demagnetization as discussed below).

Next we formulate the critical state model for the geometry of a slab of thickness D. Applied to the case $H \perp c$ with our $YBa_2Cu_3O_7$ crystal, it seems natural to consider D to be the thickness of the crystal platelet and J_c to represent that anisotropic component $J_c^{ab,ab}$ (in the notation of ref. [19]), in which currents flow in the Cu–O planes. However, recent studies [20] of crystals grown at AT&T have shown that the component $J_c^{c,ab}$ in which currents flow perpendicular to the planes is of order 30 times smaller than $J_c^{ab,ab}$. This trend has been confirmed in IBM crystals of the same type as used for the present study [20]. This means that unless the crystal is very much thinner than it is wide, the $J_c^{c,ab}$ component will dominate the critical state. Indeed, our crystal has only a 1:4 dimensional ratio for $H \perp c$. The conclusion is that the slab geometry is appropriate in our case, but with J_c interpreted as $J_c^{c,ab}$ and with D interpreted as the *long* dimension of the platelet.

Since $dB_{eq}/dH = 1$ in our model (eq. (2)), we may write Maxwell's relation for the critical state,

$$dB/dx = \pm(4\pi/c)J_c(B)\,, \tag{4}$$

where $\pm$ depends on the magnetic history (field increasing or decreasing). This equation must be solved subject to the boundary condition

$$B = H_a - H_s, \qquad H_s \equiv H_{c1} - H_b + \Delta H_{en}\,,$$

obtained by combining eqs. (2) and (3). The offset field H_s represents a combination of effects of equilibrium magnetization and surface barrier.

$H_s + H_b$ represents the flux penetration onset field we are interested in. This boundary condition is valid only for increasing applied fields where flux entry occurs. While an equation corresponding to eq. (3) can be written for decreasing applied field, it turns out not to be needed for calculation of the remanent moment at zero field.

The physics of the remanence process in the critical state model can be understood with reference to fig. 3. As the applied field is increased, flux penetrates, initially according to the $B(x)$ profile shown as the upper solid line in fig. 3a. The portion beginning at $x = 0$ can be calculated from eq. (4) to be

$$B(x) = [(H_m - H_s)^{n+1} - (n+1)Cx]^{1/n+1} \tag{5}$$

and as long as the field is not too large and the flux penetration does not reach the center, the penetration depth d (see fig. 3a) is given by

$$d = [(H_m - H_s)^{n+1} - H_b^{n+1}]/(n+1)C\,. \tag{6}$$

The flux fronts meet at the center when $d = D/2$, which defines a field H^* for full penetration,

$$H^* = H_s + H_b[1 + CD(n+1)/2H_b^{n+1}]^{1/n+1}\,.$$

When the field is reduced to zero from a maximum excursion field $H_m < H^*$, a $B(X)$ profile with opposite slope develops, ending with a density H_b at the surface in our model. By integrating the shaded area under $B(x)$ in fig. 3a, we obtain the remanent in the region $H_p < H_m < H^*$, which we call region 1:

$$4\pi M_{rem,1} = [4/(n+2)CD]\{[\tfrac{1}{2}(H_m - H_s)^{n+1} + \tfrac{1}{2}H_b^{n+1}]^{n+2/n+1} - H_b^{n+2}\}\,,$$
$$H_m < H^*\,, \qquad \text{region 1}\,. \tag{7}$$

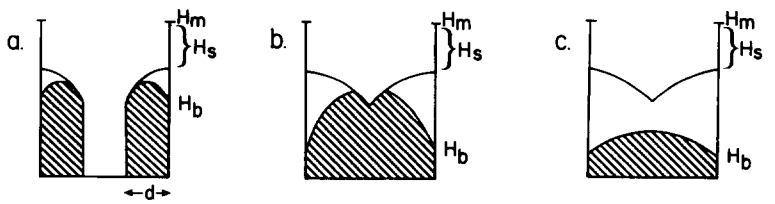

Fig. 3. Flux profiles for regions 1, 2 and 3, denoted here by a, b and c respectively; see text and eqs. (7), (9) and (10) respectively. Solid lines: Profile after turning on a field H_m. Shaded area represents the remanent magnetization after turning off the field. H_b is the height of a step function which approximates the infinite slope at H_{c1} in the $B_{eq}(H)$ – curve. The offset field H_s represents a combination of effects of equilibrium magnetization and surface barriers. $H_s + H_b$ is the flux penetration onset field H_p. For $H_s = 0$, $H_b = H_p \equiv H_{c1}$.

The remanent magnetization remains zero up to an onset at

$$H_p = H_s + H_b = H_{c1} + \Delta H_{en} , \tag{8}$$

beyond which it increases linearly and then curves upward as $\sim H_m^{n+2}/CD$. A fit of this behavior to the data will be helpful in defining the position of the onset H_p.

For H_m beyond H^*, the $B(x)$ profile enters an intermediate regime illustrated in fig. 3b. This continues until full saturation, illustrated in fig. 3c, beyond a critical field H_0. Proceeding in the same way as before, we derive the remanent moment in these regimes

$$4\pi M_{rem,2} = [2/(n+2)DC]\{2[\tfrac{1}{2}(H_m - H_s)^{n+1} + \tfrac{1}{2}H_b^{n+1}]^{n+2/n+1} - H_b^{n+2} - [(H_m - H_s)^{n+1} - \tfrac{1}{2}(n+1)DC]^{n+2/n+1}\} ,$$
$$H^* \leq H_m \leq H_0 , \qquad \text{region 2} , \tag{9}$$

$$4\pi M_{rem,3} = [2/(n+2)DC]\{[H_b^{n+1} + \tfrac{1}{2}(n+1)DC]^{n+2/n+1} - H_b^{n+2}\} ,$$
$$H_m \geq H_0 , \qquad \text{region 3.} \tag{10}$$

Because there are many parameters in these equations, we have first fitted the data taking $n = \frac{1}{2}$ and $H_s = 0$, leaving only two adjustable parameters, H_b (which in this case equals H_{c1}) and C. Examples of fits which optimally describe the region above the onset (region 1) are shown in fig. 1, with parameters listed in table I. The theory describes the onset, initial rise, rollover and saturation of the data quite well for the 20 and 35 K $H \perp c$ runs. For the 5 K run, adjusting the parameters to region 1 causes the predicted saturation value to be almost 50% too low, while for the runs above 50 K, the prediction is

Table I
Summary of the parameters used in the fits of the isothermal remanent magnetization to eq. (7) for $H \perp c$. The zero-field critical current J_c is related to C in eq. (1) via $C = J_c H_{c1}^n$. As discussion in the text, the relevant dimension in determining J_c is the long dimension, approximately 500 μm.

T (K)	H_p (Oe)	J_c (A/cm^2)
5	470	220 000
20	360	115 000
35	285	60 000
50	190	47 000
65	105	28 000

more than 50% too high. We have found that changing n and introducing a finite H_s does not substantially improve the fits. We do not know the origin of the discrepancy. A possible complication, however, might stem from a somewhat reduced Meissner effect which is found in this sample – see table of ref. [21].

Nevertheless, we have found that whatever modifications of parameters we make in our fits, the onset field for remanence is not significantly shifted as long as the initial rise in the data is fitted reasonably well. Thus we consider these onset fields H_p to be reliable, and they are plotted in fig. 4, along with points determined simply by the criterion that $M_{rem} = 0.5\,\text{emu/cm}^3$. They are also compared to points determined in the earlier study of Krusin-Elbaum et al. [5] using a different method; in the high-temperature regime ($T > 50\,\text{K}$), they agree within 25%.

We have performed a similar analysis of data taken with $H \| c$. In this configuration, demagnetizing effects dominate and recent calculations [22] have shown that there is substantial flux-line curvature in the remanent critical state. This makes a treatment based on eqs. (7)–(9) doubtful, even with the standard demagnetization correction

$$H'_m = H_m - 4\pi NM\,, \tag{11}$$

where N is the demagnetization factor (e.g. using an ellipsoidal approximation to sample shape) and M is the measured magnetization at the maximum

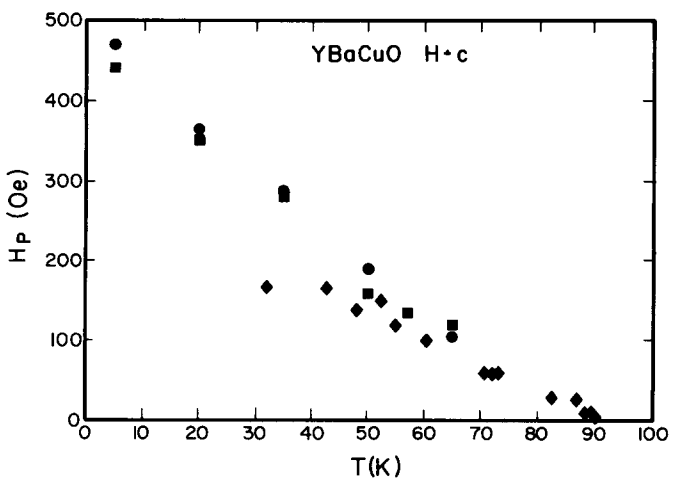

Fig. 4. Temperature dependence of the first field for flux penetration for $H \perp c$ as deduced from the field dependence of the isothermal remanent magnetization. Circles: Results of fits to eq. (7). Squares: Results of $0.5\,\text{emu/cm}^3$ criterion. For comparison we also show data points (diamonds) from Krusin-Elbaum et al. [5].

applied field. Nevertheless, we find that we can fit the remanence onset, though with the same problems in describing the saturation. Examples of fits which optimally describe the region above the onset are shown in fig. 2 with parameters listed in table II. The deduced onset fields are shown in fig. 5. We argue that at least the onset point can still be plausibly treated with a demagnetization correction since up to this point there is essentially full screening [23] and a standard demagnetizating correction has been demonstrated to work.

Table II
Summary of the parameters used in fits of the isothermal remanent magnetization for $H \| c$. The average dimension of about 500 μm is used to determine J_c, using eq. (7) without modification for the approximately square rather than slab geometry. H_p has also been corrected for demagnetization according to eq. (11).

T (K)	H_p (Oe)	J_c (A/cm^2)
5	1800	750 000
10	1600	540 000
20	1150	260 000
35	600	87 000
50	275	31 000
65	175	7 000

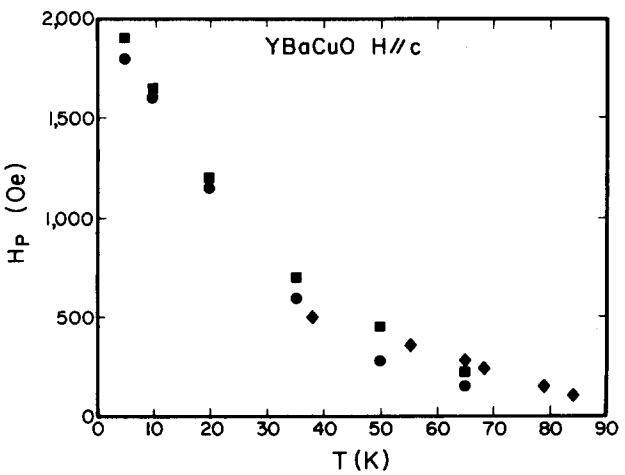

Fig. 5. Temperature dependence of the first field for flux penetration for $H \| c$ as deduced from the field dependence of the isothermal remanent magnetization. Circles: Results of fits to eq. (7). Squares: Results of 0.5 emu/cm^3 criterion. For comparision we also show data points (diamonds) from Krusin-Elbaum et al. [5].

4. Discussion

Finally, we discuss the implications of these results for H_{c1}. Basically our results confirm previous reports [8–11] showing an anomalous temperature dependence of the flux penetration field[#1]. However, there are differences in detail.

In the regime $T > 50\,\mathrm{K}$ the results are approximately linear with T, in agreement with conventional pairing models and suggesting that these indeed represent measurements of H_{c1}. Our values for $\mathrm{d}H_{c1}/\mathrm{d}T$ agree with many other reports on twinned Y–Ba–Cu–O crystals, which show a range 3–4 Oe/K for $H \perp c$ and 8–11 Oe/K for $H \| c$. By contrast, Moschalkov et al. [8] report on untwinned Tm–Ba–Cu–O crystal values of 3 Oe/K for $H \perp c$ and 20 Oe/K for $H \| c$. The large increase for $H \| c$ which they observe gives credence to their suggestion that the twin boundary planes which lie predominantly with their normals in the *ab* plane provide an easier entry point for penetrating flux and thus that the previous values for $H \| c$ are not representative of true bulk behavior[#2].

In the regime $T < 50\,\mathrm{K}$ the results paint a confusing picture. Our $H \perp c$ results lie almost a factor of two higher than those of Moshchalkov et al. and also a factor of two higher than our earlier measurements using flux creep [6]. Our $H \| c$ results give values comparable to those of Moshchalkov et al. at low temperature but twice as high as our flux creep values [6]. These variations and the anomalous temperature dependence suggest that in this regime we are *not* measuring just the intrinsic H_{c1}.

Could surface barriers make an important contribution? Our analysis in section 3 shows that the behavior of $M_{rem}(H_m)$ is rather similar whether or not surface barriers are present. The appearance of surface barriers at low rather than high temperature is plausible because the higher the temperature, the more likely the surface barrier can be overcome by thermal activation. The seemingly random variations of the onset field in this low-temperature range, summarized above, could be attributed to uncontrolled surface conditions in the different samples.

In summary, while a more positive demonstration of the surface barrier effect would be desirable, it seems a likely source for the anomalous temperature dependence, which we and others see in the flux penetration field. The claim of anomalous behavior in the lower critical field seems unwarranted at this time.

[#1] It is interesting to note that recently Shivaram et al. [24] reported on similar anomalies in UPt_3. These, however, are accompanied by related features in the upper critical fields and in the specific heat.

[#2] Recent results [25] on an untwinned Y–Ba–Cu–O crystal give a value close to 10 Oe/K for $H \| c$. This difference with results of Moshchalkov et al. is unresolved.

Acknowledgements

We wish to acknowledge important discussions with C. Schlenker, V.V. Moshchalkov, H. Fukuyama, I. Iye and T. Matsushita. This research is supported in part by the U.S.–Israel Binational Science Foundation. We particularly credit V. Moschalkov, who suggested the measuring of the time dependence of the remanence onset as a test of surface barriers.

References

[1] R.B. Goldfarb, A.F. Clark, A.I. Braginski and A.J. Panson, Cryogenics 27 (1987) 475.
[2] A. Shaulov and D. Dorman, Appl. Phys. Lett. 53 (1988) 2680.
[3] L. Fruchter, C. Giovanella, G. Collin and I.A. Campbell, Physica C 156 (1988) 69
[4] A. Umezawa, G.W. Crabtree, J.Z. Liu, T.J. Mosran, S.K. Malik, L.K. Nunez, W.L. Kwok and C.H. Sowers, Phys. Rev. B 38 (1988) 2843.
[5] L. Krusin-Elbaum, A.P. Malozemoff, Y. Yeshurun, D.C. Cronemeyer and F. Holtzberg, Phys. Rev. B 39 (1989) 2936.
[6] Y. Yeshurun, A.P. Malozemoff, F. Holtzberg and T. Dinger, Phys. Rev. B 38 (1988) 11828.
[7] Ch.J. Liu, R. Buder, C. Escribe-Filippini, J. Marcus, P.L. Reydet, B.S. Mathis and C. Schlenker, Physica C 162–164 (1989) 1609.
[8] V.V. Moschalkov, A.A. Zhukov, O.V. Petrenko, A.A. Gippins, V.I. Voronkova and V.K. Yanovskii, Proc. Dubna Conf. on High-Temperature Superconductors, Dubna, June–July (1989); V.V. Moshchalkov, O.V. Petrenko, A.A. Zhukov, A.A. Gippens, V.I. Voronkova, V.S. Belov and V.A, Rybachuk, Physica C 162–164 (1989) 1611.
[9] H. Adrian, W. Assmus, A. Höhr, J. Kowalewski, H. Spille and F. Steglich, Physica C 162–164 (1989) 329.
[10] A. Umezawa, G.W. Crabtree, K.G. Vandervoort, U. Welp, W.K. Kwok and J.Z. Liu, Physica C 162–164 (1989) 733.
[11] M. Sato, S. Shamoto, M. Sera and H. Fujishita, preprint.
[12] D.R. Harshman, L.F. Schneemeyer, J.V. Waszczak, G. Aeppli, R.J. Cava and B. Batlogg, Phys. Rev. B 39 (1989) 851.
[13] L. Krusin-Elbaum, R.L. Greene, F. Holtzberg, A.P. Malozemoff and Y. Yeshurun, Phys. Rev. Lett. 62 (1989) 217.
[14] S. Sridhar, D.W. Wu and W. Kennedy, Phys. Rev. Lett. 63 (1989) 1873.
[15] C.P. Bean and J.D. Livingston, Phys. Rev. Lett. 12 (1964) 14.
[16] C.P. Bean, Phys. Rev. Lett. 8 (1962) 250 Rev. Mod. Phys. 36 (1984) 31.
[17] L. Krusin-Elbaum, A.P. Malozemoff, D.C. Cronemeyer, F. Holtzberg, J.R. Clem and Z. Hao, J. Appl. Phys. 67 (1990) 4670.
[18] J. Clem, J. Appl. Phys. 50 (1979) 3518.
[19] D.C. Cronemeyer, T.R. McGuire, A.P. Malozemoff, F. Holtzberg, R.J. Gambino, L.W. Conner and M.W. McElfresh, Proc. Int. Conf. on Transport in High-Temperature Superconductors, R. Nicolsky, ed. (World Scientific, Singapore), in press.
[20] E.M. Gyorgy, R.B. van Dover, K.A. Jackson, L.F. Schneemeyer and J.V. Waszczak, Appl. Phys. Lett. 55 (1989) 283.
[21] L. Krusin-Elbaum, A.P. Malozemoff, D.C. Cronemeyer, F. Holtzberg, G.V. Chandrashekhar, J.R. Clem and Z. Hao, Physica A 168 (1990) 367, these Proceedings.
[22] M. Daeumling and D. Larbalestier, Phys. Rev. B 40 (1989) 9350.
[23] F.R. Sauerzopf, H.P. Wiesinger and H.W. Weber, preprint.
[24] B.S. Shivaram, J.J. Gannon Jr. and D.G. Hinks, Phys. Rev. Lett. 63 (1989) 1723.
[25] L. Krusin-Elbaum and F. Holtzberg, private communication.